Ocean and atmosphere feedbacks affecting AMOC hysteresis in a GCM

Article

Accepted Version

Climate Dynamics manuscript No.
(will be inserted by the editor)

Ocean and Atmosphere feedbacks affecting AMOC hysteresis in a GCM

L.C. Jackson · R.S. Smith · R.A. Wood

Received: date / Accepted: date

Abstract Theories suggest that the Atlantic Meridional Overturning Circulation (AMOC) can exhibit a hysteresis where, for a given input of fresh water into the north Atlantic, there are two possible states: one with a strong overturning in the north Atlantic (on) and the other with a reverse Atlantic cell (off). A previous study showed hysteresis of the AMOC for the first time in a coupled general circulation model (Hawkins et al, 2011).

In this study we show that the hysteresis found by Hawkins et al (2011) is sensitive to the method with which the fresh water input is compensated. If this compensation is applied throughout the volume of the global ocean, rather than at the surface, the region of hysteresis is narrower and the off states are very different: when the compensation is applied at the surface, a strong Pacific overturning cell and a strong Atlantic reverse cell develops; when the compensation is applied throughout the volume there is little change in the Pacific and only a weak Atlantic reverse cell develops.

We investigate the mechanisms behind the transitions between the on and off states in the two experiments, and find that the difference in hysteresis is due to the different off states. We find that the development of the Pacific overturning cell results in greater atmospheric moisture transport into the North Atlantic, and also is likely responsible for a stronger Atlantic reverse cell. These both act to stabilize the off state of the Atlantic overturning.

Keywords MOC · THC · hysteresis

L.C. Jackson
Met Office Hadley Centre, Exeter, UK.
Tel.: +44 1392 885680
Fax: +44 1392 885681
E-mail: laura.jackson@metoffice.gov.uk

1 Introduction

One of the open questions in climate studies is whether the Atlantic Meridional Overturning Circulation (AMOC) has the potential to collapse in present day and future climates. Paleoclimate studies (Rahmstorf, 2002; McManus et al, 2004; Clement and Peterson, 2008; McNeall et al, 2011) have shown that rapid changes in surface climate have occurred in the past and that these may have been caused by a switch from a vigorous Atlantic overturning ('on' state) to a weak or reversed overturning ('off' state). Although a collapse of the AMOC has been judged to be very unlikely within the 21st century based on projections of future climate change by current general circulation models (GCMs) (Collins et al, 2013), such a collapse would have large impacts on the climate (Vellinga and Wood, 2008; Kuhlbrodt et al, 2009; Jackson et al, 2015). Hence it is important to understand what determines the stability of the AMOC and the processes behind a collapse in order to make an assessment of the likelihood of a collapse occurring in the future.

Simple box models of the overturning circulation have shown that there are theoretical reasons for believing that rapid shifts between MOC states are possible (Stommel, 1961; Rahmstorf, 1996). These models show that for a range of additional fresh water input into the sinking regions (as might occur from melting ice sheets, or from an increased hydrological cycle) there are two possible stable states (bistability) for the AMOC. This results in potentially irreversible transitions (hysteresis) between overturning states when the climate is altered. The process responsible for this bistability is a positive salt advection feedback whereby a decrease in the AMOC strength results in less northwards transport of salt and therefore a freshening of the North Atlantic and a further weakening of the AMOC. In more complex ocean and coupled climate models this feedback is expected to still play a role, however biases in salinity can remove, or even reverse this feedback and other feedbacks can also be important (Schiller et al, 1997; Vellinga et al, 2002; de Vries and Weber, 2005; Jackson, 2013). Many GCMs previously had biases that did not allow for a positive salt advection feedback (Drijfhout et al, 2011), however this bias has been removed in some current GCMs (Weaver et al, 2012).

Many studies (for example Rahmstorf et al, 2005; Hofmann and Rahmstorf, 2009; Weber and Drijfhout, 2007; Cimatoribus et al, 2012) have shown that the hysteresis and bistability shown in the box models still exists in more complex climate models with dynamic oceans (either forced ocean only models, Earth System Models of Intermediate Complexity (EMICs) or simpler models), and in a coupled Atmosphere-Ocean general circulation model (Hawkins et al, 2011, discussed below). The range of fresh water input for which there are bistable states has been found to be model dependent due to factors including mixing strengths and parameterizations, wind stress, model biases and atmospheric feedbacks (Rahmstorf et al, 2005; Hofmann and Rahmstorf, 2009; Sévellec and Fedorov, 2011).

There are substantial differences in AMOC off states between models. There are theoretical reasons to expect that wind-driven upwelling in the

Southern Ocean should be balanced globally by sinking somewhere when in a steady state (Kuhlbrodt et al, 2007; de Boer et al, 2008), however the wind-driven upwelling can be counteracted by eddy-induced transports in the Southern Ocean, eliminating or reducing the requirement for high latitude deep water formation (Johnson et al, 2007). Some model studies have found off states with no northern hemispheric sinking and with reversed overturning cells in the Atlantic(Marotzke and Willebrand, 1991; Manabe and Stouffer, 1999; Gregory et al, 2003). Others have found deep water being formed instead in the Pacific forming a Pacific Meridional Overturning Circulation (PMOC) cell (Marotzke and Willebrand, 1991; Saenko et al, 2004).

Saenko et al (2004) describe an 'Atlantic-Pacific seesaw'. They used an EMIC and found that by adding fresh water to the Atlantic they caused a shutdown of the AMOC and a more gradual strengthening of the PMOC. They also showed that they could make the AMOC collapse by removing fresh water from the Pacific which caused a more rapid strengthening of the PMOC. The link between the two basins was suggested to be an advective feedback of salinity. Other studies have also found a strengthening of the PMOC following reduction or cessation of the AMOC. Mikolajewicz et al (1997) found that a reduction of the AMOC caused cooling of the North Pacific from a reduced northwards Atlantic ocean heat transport. This together with wind shifts over the North Pacific resulted in increased convection and the formation of North Pacific intermediate water. Okazaki et al (2010) also found that a shutdown of the AMOC caused changes in surface fresh water fluxes in the Pacific, with a northwards shift of the Intertropical Convergence Zone (ITCZ) and reductions in tropical atmospheric water transport from the Atlantic to Pacific resulting in a more saline North Pacific and deep water formation in the North Pacific. Sinha et al (2012) showed that the switch between Atlantic and Pacific overturning can also be achieved by changes in the atmospheric transport of fresh water. They conducted an experiment with an EMIC with no mountains in North America, resulting in a greater fraction of the atmospheric fresh water originating from the Pacific falling as precipitation in the Atlantic, rather than over mountain ranges and being returned to the Pacific as river runoff. The result was a fresher Atlantic, saltier Pacific and overturning predominantly in the Pacific.

The existence of the Atlantic-Pacific seesaw may be sensitive to the geographic representation however. Hu et al (2012) showed that adding freshwater to the Atlantic caused a decrease in the the AMOC and a strengthening of the PMOC in a GCM. However they also found that there was much less response of the PMOC to an AMOC shutdown when the Bering Straits was open rather than closed. This is because an open Bering Straits allows a pathway for fresh North Atlantic/Arctic water to reach the Pacific and reinforce the halocline. Paleoclimate data studies have suggested that there may have been various periods in the past where the PMOC was stronger than currently (Thomas et al, 2008; Holbourn et al, 2013; Menviel et al, 2014) including Okazaki et al (2010) who suggested that there was a shift between the AMOC and PMOC during the Last Glacial Termination.

Hawkins et al (2011) conducted the first hysteresis experiment using a coupled GCM (FAMOUS, Smith et al, 2008). They first conducted transient experiments, where fresh water hosing into the Atlantic increased and then decreased linearly, which showed a hysteresis (different values during the ramp up and down of hosing). They then spun off a few experiments with constant hosing values to identify equilibrium states (Fig 1a). This showed a narrower range of hosing values with bistability (two different stable states) of the AMOC (Fig 2). In those experiments the Atlantic hosing was compensated by a uniform removal of fresh water from the surface over the rest of the ocean. We will refer to this set of experiments as SCOMP. Using an alternative experimental design (VCOMP, in which the hosing compensation was applied over the full ocean volume) there is a much narrower hysteresis loop and no evidence of bistability (Fig 1b). (Note that in this study we will use hysteresis to refer to the different AMOC strengths during the transient experiment where hosing is increased and decreased, and reserve bistability for the discussion of equilibrium states.) The hosing is the same in both experiments with the only difference being the way in which the compensation to the hosing is applied, hence the difference must be ultimately caused by the different hosing compensation strategies. There is also a fundamental difference in the way in which the Pacific responds. In SCOMP an increase in hosing results in a strong Pacific Meridional Overturning Circulation (PMOC) which also exhibits both hysteresis and bistability (Fig 1c), however there is very little response of the PMOC in VCOMP (Fig 1d).

This raises several questions which will be addressed here. After presenting the methods (section 2) we will investigate the overturning in more detail (section 3). We will then investigate why the hysteresis loop is wider in SCOMP than VCOMP which can be broken down into two questions: why does the AMOC in SCOMP stay strong for longer when hosing is increased (black lines in Fig 2; discussed in section 4)?; and why does the AMOC in SCOMP stay weak for longer when hosing is decreased (gray lines in Fig 2; discussed in section 5)? We do not directly investigate the difference in bistability of the two experiments, but hypothesize that the mechanisms that result in the on and off states of the AMOC in SCOMP being more resistant to change during the hysteresis, are also important in maintaining the stable on and off states. We will also investigate why there is a strengthening of the PMOC in SCOMP but not VCOMP and show that this is connected to the different behavior of the AMOC (section 6), and discuss the role played by atmospheric transports (section 7). Conclusions are presented in section 8.

2 Methods

We analyze several experiments using the FAMOUS (Smith et al, 2008) GCM. FAMOUS is a low resolution, retuned version of the third Met Office Hadley Centre GCM (HadCM3) (Gordon et al, 2000) The atmospheric component

has a horizontal resolution of 5^o x 7.5^o, with 11 vertical levels, and the ocean component has a horizontal resolution of 2.5^o x 3.75^o, with 20 vertical levels.

Both this study and Hawkins et al (2011) use version XDBUA of FAMOUS. Amongst other factors, FAMOUS differs from HadCM3 in that it does not use the deeper overflow channels created in HadCM3 to increase the flow of dense water through the Denmark Straits, and uses the local surface salinity to transform surface freshwater forcing into the virtual salt flux required by its rigid lid ocean formulations. Although the Bering Straits are open in the model, the configuration of the rigid lid enforces zero net mass flux through them, significantly restricting the tracer transport that can occur through the Straits. FAMOUS does not require flux adjustments for stability, but a time-invariant pattern of freshwater flux is added to the ocean which represents iceberg melting to compensate for the perennial build up of snow on land in the polar regions at a rate diagnosed from a control run.

Analysis is performed on two experiments, including one which was carried out as part of the study by Hawkins et al (2011), where fresh water flux (hosing) was applied over the North Atlantic (20-50^{o}N). To prevent salinity drift over long timescales, fresh water must be conserved within the ocean. This was done by two different methods: firstly SCOMP uses a surface compensation where fresh water is removed over the ocean surface outside of the hosing region; secondly VCOMP uses a volume compensation where the compensation for the hosing is applied over the whole volume of the ocean by removing fresh water from each grid point. For both designs there were initial transient experiments where the magnitude of the hosing flux was ramped up slowly (increasing linearly from 0 to 1 Sv over 2000 years, ie 5e-4 Sv/yr) and then ramped down at the same rate to 0 Sv (see Fig. 1). Hawkins et al (2011) found in SCOMP that there are a range of values of the hosing where there were both on and off AMOC states. Constant hosing experiments (where the fresh water flux was kept constant for a number of years) were then spun off from both on and off states to find the 'equilibrium' states. Hawkins et al (2011) describe the initial hysteresis experiment and spin off equilibrium experiments in more detail.

The MOC in the Atlantic and Indo-Pacific are measured at 26^{o}N, 798m though these indices are representative of the changes over the MOC cell. Anomalies are taken with respect to the on state (time mean of the first 200 years of the hosing ramp up experiment) or to the off state (time mean of the first 200 years of the hosing ramp down experiment) as indicated.

3 The global overturning circulation

The initial state (before hosing is applied) in SCOMP and VCOMP consists of a strong Atlantic Meridional Overturning Circulation (AMOC), characterized by sinking of North Atlantic Deep Water (NADW), and a weak Antarctic bottom water (AABW) cell where bottom waters produced in the Antarctic mix with the NADW cell and are returned at a shallower depth (Fig 3a). In the

Pacific there is a strong cell upwelling bottom water, but there is no Pacific Meridional Overturning Circulation (PMOC) with sinking of North Pacific deep water analogous to that in the North Atlantic (Fig 3b).

As shown in Hawkins et al (2011), after 2000 years of hosing in SCOMP the AMOC cell has vanished and been replaced by a strengthened AABW cell (Fig 3c). There are also indications of a shallow (upper 1000m) Antarctic Intermediate water (AAIW) cell. The circulation has also changed in the Pacific, with the formation of a vigorous PMOC cell (Fig 3d). Both the overturning in depth and density space (Fig 3d,4e) show the circulation weakening and becoming shallower/less dense as it moves southwards, suggesting diffusive upwelling. The greater upwelling in the Pacific basin may be because there is a greater area of the ocean over which diffusive upwelling can occur.

The final state in VCOMP is very different from that in SCOMP, despite experiencing the same rate and length of hosing. Although the AMOC has disappeared and there is a reverse AAIW cell, the off state consists of a much weaker reverse cell (Fig 3e). The Pacific state is also very different with no deep sinking occurring in the North Pacific and only a weak, shallow PMOC cell, although the upwelling of Pacific bottom water is weaker (Fig 3f).

The mechanisms behind the collapse of the AMOC and strengthening of the PMOC are discussed in future sections, however there is less known about what controls the reverse cells. In steady state the formation of dense water must be balanced globally by upwelling/lightening of water elsewhere. This occurs through diapycnal mixing and through a wind-driven upwelling in the southern ocean that is at least partially compensated by eddies (Kuhlbrodt et al, 2007; Johnson et al, 2007; de Boer et al, 2008). It appears plausible that the water upwelled by the reverse PMOC/AMOC cells could be the return branch of the strong AMOC/PMOC cells, however when regarding these cells in density space (Fig 4) it can be seen that the waters upwelled in the reverse cells are denser than the deep waters leaving the other basin. The water being upwelled is therefore AABW and forms an AABW cell. The strength of this cell globally is similar in both on and off states of SCOMP (Fig 4c,f) however the partition between the upwelling in the Atlantic and Pacific basins changes, with greater upwelling in the basin without a vigorous overturning circulation. The presence of dense water formed in the North Atlantic or Pacific reduces the meridional density gradient at depth in that basin. We hypothesize that this density gradient impedes the northward transport of AABW, resulting in greater upwelling in the basin without deep water formation. In VCOMP once the AMOC has collapsed there is no deep water formed in the North Pacific allowing a greater upwelling there. The strength of the AABW cell is reduced, which is possibly due to an increase in stratification in the Southern Ocean. This increase in stratification in VCOMP is caused by a freshening in surface layers and salinification in the deep ocean, likely as a result of adding fresh water to the surface north Atlantic and removing it throughout the depth of the ocean.

Although the overturning circulations change substantially in both basins, the global overturning at 30^oS remains very similar (Fig 3g,h). This suggests

that the global overturning is set by some other constraint, such as the wind-driven upwelling in southern ocean. This is consistent with the results from Schewe and Levermann (2010) who found that the total volume export from the Atlantic and Pacific below 780m was controlled by the southern ocean wind stress, but that the split between the Atlantic and Pacific was controlled by regional densities. Our experiments and those of Schewe and Levermann (2010) all use resolutions at which eddies must be parameterized (with the Gent-McWilliams scheme in FAMOUS; Gent and McWilliams, 1990), however an eddy resolving model might experience larger changes in eddy-driven compensation in the southern ocean which would change the total wind-driven upwelling there.

3.1 Controls on the AMOC and PMOC

Previous studies have shown that the AMOC strength can be related to a meridional density gradient in the Atlantic (Thorpe et al, 2001; Schewe and Levermann, 2010; Roberts et al, 2013). Fig 5a shows that this holds in these experiments and that the relationship between meridional density gradient and the AMOC is the same across all the experiments. A similar relationship is also found between the PMOC and a meridional density gradient in the Pacific (Fig 5c). The density changes mainly occur in the North Atlantic and Pacific, with little density change in the southern boxes. The meridional density difference changes by 0.3 kg/m^3 between the MOC on and off states in the Atlantic, and by 0.2 kg/m^3 in the Pacific. These density changes can be explained by the salinity-driven changes in the northern boxes only (Fig 5b,d). There are smaller temperature-driven density changes, particularly in the Pacific, however these tend to offset the salinity-driven changes.

These relationships between the overturning circulations and the salinities in the northern Atlantic and Pacific, suggests that the key to understanding the behavior of the overturning circulation is to investigate the evolution of the salinity in the two basins.

4 The AMOC 'on' branch

To investigate why there is a greater hysteresis in SCOMP we first examine the ramp up experiment, where the hosing is increased slowly from 0-1Sv. In SCOMP the AMOC decreases little until a hosing value of ≈ 0.45 Sv is reached. Then there is a more rapid decrease of the AMOC (Fig 2, 6a). In contrast the AMOC in VCOMP starts decreasing earlier and decreases more steadily. Both, however, reach a state where the AMOC is off at about the same hosing value of 0.55 Sv.

To understand this difference in the behavior, we show the budget terms for the North Atlantic ($40-90^o$N) salinity in Fig 6. This salinity behaves in the same way as the AMOC with that for VCOMP decreasing more initially, followed by an accelerated decrease in SCOMP (Fig 6b,c). The budget comprises

surface fluxes into the north Atlantic (which freshen the region) and advective fluxes (which salinify the region). The advection can be split into components due to the overturning circulation and the horizontal or gyre circulation, as well as parameterized mixing.

In both SCOMP and VCOMP there is a freshening from hosing over the first 800 years (seen in the surface fluxes, Fig 6d) which is partly compensated by increasing advection from the gyre component (cyan line in Fig 6e). VCOMP freshens more because it experiences a greater reduction in advection of salt from the overturning circulation (green lines in Fig 6e,f). A decomposition of the overturning component into contributions from changing salinities and changing velocities shows that both contribute for the first 650 years, with the latter taking over from years 650-800. The greater contribution from velocity changes can be explained by the greater weakening of the AMOC in VCOMP, however this does not identify a cause for the greater weakening. The salinity contribution, on the other hand, can be explained by the difference in experimental design. In SCOMP, the compensation to the hosing (ie removal of fresh water) is applied to the surface ocean, whereas in VCOMP it is applied throughout the ocean volume. This results in increasingly saline water in the surface ocean outside the hosing region in SCOMP (Fig 7). This more saline water is advected into the hosing region by the mean circulation and retards the AMOC reduction.

Although the AMOC in SCOMP stays relatively stable for the first 800 years, there is then an accelerated decrease (Fig 2a). This initially occurs because of an accelerated freshening from increased fresh water input from surface fluxes (red lines, Fig 6d,f) followed by positive advective feedback as the circulation changes (green lines, Fig 6e,f). The additional changes to surface freshwater fluxes will be shown (Section 7) to be from increased precipitation over the subpolar and polar north Atlantic and to be associated with the strengthening of the PMOC in SCOMP.

In summary the salinity, and therefore the AMOC, in VCOMP has an accelerated decrease because of an advective feedback (the weakening AMOC transports less salt into the convection region which further weakens the AMOC). In SCOMP, on the other hand, this feedback is inhibited by the increasing salinity of the surface water (from the surface hosing compensation) advected northwards, until an increased fresh water input from precipitation from year 800. Hence the cause of the AMOC staying stronger for longer in SCOMP than VCOMP is the form of the hosing compensation. However since the AMOC reaches an off state at similar values of hosing in SCOMP and VCOMP, the difference in width of the hysteresis loop is more strongly dependent on the AMOC recovery.

5 The AMOC 'off' branch

When reducing the hosing the AMOC stays in its off state until the hosing reaches 0.5 and 0.3 Sv for VCOMP and SCOMP respectively (Fig 2). Since

the AMOC stays off longer in SCOMP the hysteresis curve is wider. Before the AMOC starts increasing there is a reduction in the AAIW cell (measured as the minimum streamfunction at 30^oS over 200-800m depth), with the disappearance of the AAIW cell occurring at the same time as the AMOC starts increasing (Fig 8a). The AABW cell (measured as the minimum streamfunction at 30^oS below 3000m depth) changes little in VCOMP and weakens in SCOMP only when the AMOC starts recovering.

Reducing the hosing results in an increase in salinity and hence density of the north Atlantic in both experiments, with the AMOC only starting to increase once the densities of the north and south Atlantic boxes become comparable (Fig 8b). The reversal of the meridional density gradient and hence recovery of the AMOC happens earlier in VCOMP because the salinity of its northern box increases faster, particularly over the first 1200 years. Saline anomalies (relative to the very fresh North Atlantic water in the off state) form over the hosing region (20-50^oN). This region is also the source of the difference in salinity between the two experiments. Hence we extend our region for the budget analysis to 20-90^oN, although results with the original region (40-90^oN) are similar.

There are differences between the off state budgets (Fig 8): In SCOMP there is a greater surface input of fresh water into the North Atlantic than in VCOMP, and this is balanced by a greater export of fresh water, which is due to a greater export by the stronger reverse Atlantic cell (Fig 3). A contribution to the greater surface input of fresh water will be shown (Section 7) to be from more precipitation and associated with the PMOC cell in SCOMP.

As the hosing reduces, the North Atlantic in both experiments becomes more saline, although this is partly mitigated by a reduction in the export of fresh water. VCOMP, however, has a faster salinification (Fig 8c). The reduction in hosing occurs at the same rate in the two experiments and there is little change in the net precipitation (precipitation minus evaporation) over the first 1200 years, so the difference in surface fluxes remains relatively stable (red lines in Fig 8d,f). The greater salinification instead occurs because the export of fresh water in VCOMP decreases more slowly than the export of fresh water in SCOMP (blue lines in Fig 8e,f). In particular the differences in advection come from the different advection of salinity anomalies by the off state overturning circulation (green dashed line in Fig 8f).

The key to understanding the different salinity recovery lies in the different off states. In SCOMP there is a greater input of fresh water from surface fluxes, balanced by a greater export of fresh water by the stronger overturning circulation. When the hosing, and therefore the fresh water input from surface fluxes decreases, this results in a saline anomaly relative to the previously very fresh surface Atlantic water. The stronger overturning circulation in SCOMP is more effective than that in VCOMP at removing this anomaly and hence retaining the fresh surface waters. Hence the surface salinity in the North Atlantic increases faster in VCOMP than SCOMP. This can be understood more clearly with the aid of a simple box model as shown in the Appendix.

The increased surface salinity reduces stratification and encourages deep convection and the recovery of the AMOC. Once the AMOC starts increasing there is a positive advective feedback whereby more saline water is advected into the region by the AMOC (green lines in Fig 8e), further salinifying the North Atlantic. A study of the decrease and resumption of the Atlantic overturning found that these positive advective and convective feedbacks can cause a rapid increase in the AMOC strength and even an overshoot (Jackson et al, 2013). Fig 2 shows some overshoot of the AMOC as it recovers in both experiments.

In summary, the two models respond differently to reducing the hosing because of their different off states. SCOMP has a stronger reverse cell which is more efficient at exporting salinity anomalies, and hence is more stable than that in VCOMP. This results in a wider hysteresis curve.

6 The PMOC

The overturning circulation in the Pacific behaves very differently in the two experiments, with SCOMP developing a strong Pacific Meridional Overturning Circulation (PMOC), whereas no such circulation develops in VCOMP (Fig 2,3 and 4). In SCOMP the PMOC starts increasing properly around year 800 (Fig 9), however there is a slight increase in both the north Pacific salinity and the PMOC prior to this. Since this salinity increase is predominantly in the surface Pacific (Fig 7c), the volume average salinity change is very small and difficult to attribute using a budget analysis (not shown). Once the PMOC starts increasing there are feedbacks that result in the salinity and PMOC increasing more rapidly (Fig 9a,b). It is the initial salinification in the surface Pacific, however, that triggers the increase of the PMOC.

The salinification of the North Pacific can be attributed to the surface compensation of the hosing flux. Although the fresh water removed from the North Pacific is an order of magnitude smaller than the fresh water added in the North Atlantic, it can still have a significant impact on the Pacific. After 500 years there has been a total hosing input of 62.5 Sv yr into the surface Atlantic and an equivalent removal of fresh water from the compensation everywhere else. Applying this compensation over the upper 1000m would result in an increase in salinity of approximately 0.2 PSU, consistent with the salinity change seen in the upper waters of the North Pacific in SCOMP (Fig 7).

The salinification of the surface North Pacific erodes the halocline there, making the water column less stable and encouraging deep convection. Various studies have found that removing fresh water from the surface North Pacific can result in a strengthening of the PMOC (Saenko et al, 2004; Menviel et al, 2012). Fig 9d shows the increasing salinity of the upper North Pacific over the first 800 years. Towards the end of this period there are indications of increased vertical mixing as the subsurface warm layer (200-800m) cools and the water above and below warms (Fig 9c,10a) . This becomes more prominent after year 800 indicating a large increase in deep convection which brings warm,

salty, subsurface water to the surface. Also the strengthening PMOC advects more warm and salty water from the tropics (not shown). These both result in the increased salinification and warming of the North Pacific and further intensification of the PMOC.

In summary, the PMOC becomes strong in SCOMP because the fresh water removal by the hosing compensation reduces the stratification in the Pacific and can encourage deep convection to start. It should be noted that the Pacific in FAMOUS contains biases that could affect these processes. In particular the subsurface warm and salty water seen in the unperturbed model state is not present in the present day climatology (see Fig. 10). This means that the Pacific in our model experiments is more sensitive to changes that can initiate the convective feedbacks and cause an increase in PMOC strength than the present day climate.

7 An atmospheric bridge

In VCOMP, where the AMOC is reduced but PMOC changes little, the impacts on surface fresh water fluxes are similar to previous studies where the AMOC is reduced (Vellinga et al, 2002; Krebs and Timmermann, 2007; Yin et al, 2006). In particular the reduced northwards heat transport in the Atlantic results in colder temperatures in the North Atlantic and warmer in the South Atlantic. This reduces (increases) the evaporation over the North (South) Atlantic, resulting in less (more) atmospheric moisture and therefore less (more) precipitation (Fig 11e,h). The reduction in northwards heat transport also moves the latitude of maximum sea surface temperature southwards, resulting in increased (decreased) precipitation south (north) of the equator in the Atlantic (a southwards shift of the Atlantic Inter-tropical Convergence Zone; ITCZ).

We might expect that a strengthening of the PMOC would have the opposite results in the Pacific. Comparing SCOMP (which has a strong PMOC) with VCOMP (which does not) we indeed see increased evaporation and precipitation over the North Pacific (consistent with the warmer temperatures seen in Fig 9c) and a northwards shift of the Pacific ITCZ (Fig 11f,i). This is also consistent with the study of Lenton et al (2007) which found similar impacts from the appearance of a PMOC cell. The presence of the PMOC has effects outside the Pacific alone. In particular there is increased precipitation throughout the North Atlantic and Arctic in SCOMP compared to VCOMP (Fig 11f). We suggest that this increased precipitation is a result of increased transport of atmospheric moisture from the Pacific (where there is greater evaporation because of the strong PMOC in SCOMP, Fig 11i).

Fig 12 shows the vertically integrated atmospheric moisture fluxes along with their divergences. The divergences show the gain of fresh water by the atmosphere (assuming little storage in the atmosphere) and hence the fresh water loss by the ocean, and are multiplied by -1 to compare with the net flux into the ocean. When the AMOC has collapsed (and PMOC strength-

ened in SCOMP) there is a greater transport of atmospheric moisture across North America in SCOMP than VCOMP (Fig 12c,d). Moisture from the more strongly evaporative North Pacific is transported northeastwards, with much falling over Canada and Alaska (with some draining into the Arctic and Atlantic), and some crossing the continent to the subpolar North Atlantic and Arctic. There is also a greater transport of fresh water across the southern USA.

The budget for the North Atlantic salinity also showed an increased input of fresh water whilst the AMOC was collapsing in SCOMP (Section 4, Fig 6). This input of fresh water accelerated the salinity, and AMOC, decrease. Time series of fresh water fluxes over a similar Atlantic region (Fig 12e) also shows the increase in fresh water input from year 800. In both SCOMP and VCOMP we see the reduction in evaporation and precipitation as the AMOC decreases as previously discussed. In SCOMP, however, the precipitation first increases at year 800 before decreasing, resulting in more fresh water input than VCOMP for the rest of the simulation. This increase in precipitation occurs at the same time as the increase in evaporation in the Pacific (Fig 12f). Atmospheric moisture fluxes also show a path from the evaporative region in the North Pacific to the subpolar North Atlantic at this time (Fig 12c). This all suggests that the strengthening of the PMOC at year 800 (discussed in Section 6) causes a greater transport of fresh water to the North Atlantic via an atmospheric bridge between the Pacific and Atlantic. It is this fresh water input that then initiates the accelerated AMOC decrease seen in SCOMP (discussed in Section 4).

In Section 5 it was shown that the two off states differ with SCOMP having a greater input of fresh water into the Atlantic, which is balanced by a greater export of fresh water from the stronger reverse cell. This greater fresh water input is mainly from greater precipitation (Fig 12e) with a contribution from the greater transport of moisture from the North Pacific to the North Atlantic by the atmosphere (Fig 12d). This shows one way in which the Atlantic state is connected to the Pacific state.

In summary, a increase of the PMOC results in greater northwards heat transport and hence greater evaporation in the North Pacific. There is evidence for this resulting in a greater atmospheric transport of moisture from the North Pacific to North Atlantic and Arctic basins, and hence causing a freshening of the North Atlantic. It should be noted that there is a bias in the atmospheric moisture transport in FAMOUS, which has a greater transport across North America than in the ERA interim reanalysis Dee et al (2011) (Fig 12a,b). Hence this atmospheric link between the two basins could be weaker than found in this model, nevertheless it does show the potential for the Pacific MOC to influence the Atlantic MOC via an atmospheric bridge.

8 Conclusions

Two different hysteresis experiments (where an additional fresh water flux in the North Atlantic is gradually increased and then decreased) show very different impacts on the overturning circulation, particularly in the Pacific. When the fresh water addition is compensated by removing fresh water from the global ocean surface (SCOMP), the overturning circulation responds with the formation of a deep overturning cell in the Pacific and a strong reverse cell upwelling in the North Atlantic. On the other hand, when the fresh water addition is compensated throughout the ocean volume (VCOMP), there is little response in the Pacific, and the reverse cell in the Atlantic is much weaker. In SCOMP a greater reduction of fresh water input is required before the AMOC recovers to its original state, so the hysteresis is wider. This is shown to be caused by the differences in the reverse Atlantic cell which is stronger in SCOMP than in VCOMP.

The ultimate reason for the two experiments having different off states, however, is the way in which the compensation is applied. In SCOMP, the compensation makes the surface Pacific more saline, decreasing stratification and encouraging deep convection. This results in the development of a Pacific overturning cell, which has two impacts on the Atlantic. Firstly the Pacific overturning warms the surface Pacific, resulting in increased evaporation, an increased atmospheric moisture transport across North America, and greater precipitation in the North Atlantic. This fresh water input into the North Atlantic impedes the formation of deep water and helps to maintain an AMOC off state. Also, greater sinking in the North Pacific may result in less transport of AABW into the Pacific and hence a greater upwelling of AABW in the Atlantic, resulting in the stronger Atlantic reverse cell. This reverse cell also helps to maintain an AMOC off state by being more stable to salinity changes.

The markedly different results when using different hosing compensations raises the question of which is the best to use. Surface compensation is the most realistic if the scenario considered is that where surface fluxes are changing, although these are unlikely to be evenly distributed in reality. The addition of fresh water into the north Atlantic is normally considered to be an idealization of fresh water input from melting ice sheets. In reality that would require no compensation, but would require an increase in global mean sea level and a reduction in global mean salinity. Since most general circulation models cannot simulate an increase in the volume of the ocean, volume compensation could be justified in that it has the least impact on the salinity distribution elsewhere, and might be the most appropriate compensation to use when equilibrium solutions (where the global mean salinity is not changing) are sought.

The results presented here show that the nature of the off state reached (eg the presence of a Pacific overturning, the nature of the Atlantic reverse cell, atmospheric teleconnections) can be very important in determining the hysteresis. We hypothesize that the mechanisms that control the differences in AMOC collapse and recovery during the transient hysteresis experiments are also important in determining the relative stability of the equilibrium on

and off states. Hence the nature of the off state reached may have important implications for the presence of bistability.

Previous studies (Marotzke and Willebrand, 1991; Manabe and Stouffer, 1999; Gregory et al, 2003; Saenko et al, 2004) have found hysteresis and bistability in other models with different off states (including without a Pacific overturning cell), hence the nature of the stable off state might be model dependent. It is unclear whether the different results found in FAMOUS are a result of its greater complexity, or due to model biases or the hosing methodology, however we note that simple models which do not allow changing atmospheric fresh water transports between the Atlantic and Pacific would not be able to reproduce the results found in SCOMP. It also is possible that these results might be resolution dependent; Mecking et al (2016) found that freshwater advection by eddies in an eddy-permitting model can be important in the AMOC recovery. Despite the possible model dependence of these results, they do suggest that it is not sufficient to have no AMOC cell for a stable off state, and that the presence of a strong reverse Atlantic cell and a PMOC cell can help to stabilise the off state.

Acknowledgements This work was supported by the Joint UK DECC/Defra Met Office Hadley Centre Climate Programme (GA01101). This work was also partly funded by NCAS-Climate. The simulations were performed on HECToR, the UK National Supercomputing Service in 2009.

9 Appendix: Box model of AMOC recovery

When the hosing is reduced over the North Atlantic, in both SCOMP and VCOMP the salinity recovers from that in the AMOC off state, with saline (less fresh) anomalies appearing in upper 500m of the region in which the hosing is applied. The salinity in VCOMP recovers faster. To illustrate why we consider a simple model where the upper North Atlantic is represented by a box with volume V (m^3) and salinity S (PSU). A circulation of strength Q (m^3/s), representing the reverse overturning cell, imports water of salinity $S_0 > S$ (PSU). There is a surface fresh water flux F (m^3/s of fresh water) from precipitation minus evaporation plus hosing. Hence the salinity budget of the box can be written

$$V\frac{dS}{dt} = Q(S_0 - S) - FS.$$

In steady state

$$\overline{Q}(S_0 - \overline{S}) = \overline{F}\ \overline{S}.$$

Now as the hosing input decreases, so does F, so we set $F = \overline{F} - h$ where h represents the hosing decrease. The salinity in the box increases from that in the off state as $S = \overline{S} + \sigma$ and the circulation changes $Q = \overline{Q} - q$ where we make the assumption that the circulation decreases as the salinity in the box (and hence density in the north Atlantic) increases (such as in Fig 8b), so that

$q = \beta\sigma$. Hence we have (assuming that the changes in salinity are small and hence neglecting σ^2 and σh terms)

$$V\frac{d\sigma}{dt} = -(\overline{Q} + \overline{F} + \beta(S_0 - \overline{S}))\sigma + h\overline{S}$$

or

$$\frac{d\sigma}{dt} = -\frac{1}{\tau}\sigma + H$$

where $\tau = V/(\overline{Q} + \overline{F} + \beta(S_0 - \overline{S}))$ and $H = h\overline{S}/V$. The timescale τ can be thought of as a residence time for salinity anomalies within the region.

The solution for this with $H = \lambda t$ (the hosing reducing linearly with time) using $\sigma = 0$ at $t = 0$ is

$$\sigma = \lambda\tau^2\left(e^{-t/\tau} - 1 + t/\tau\right)$$

To compare this to our model experiments we need to calculate the timescale τ and hosing reduction λ for both SCOMP and VCOMP. We assume that the changes in advection are dominated by the advection of salinity anomalies by the mean flow so that $\tau = V/(\overline{Q} + \overline{F})$. This is true initially in experiments (Fig 8f), however we note that allowing the reverse cell to decrease would reduce the timescale. We also ignore the contribution of advection by a gyre circulation which would increase the value of $\overline{Q}$ and hence also reduce the timescale. These assumptions are made to allow a comparison with the model and to illustrate the impact of the different off states on the salinification of the North Atlantic.

Using a box from 20-60^{o}N and up to 500m deep we calculate the volume $V = 3.5 \times 10^{15}\mathrm{m}^3$ and the salinification by surface fluxes $\overline{F}$ to be 6.6×10^5 and $7.0 \times 10^5\mathrm{m}^3/\mathrm{s}$ for VCOMP and SCOMP respectively. We also estimate $\overline{Q}$ from the overturning cell strength at 20^{o}N to be 3.0×10^6 and $4.0 \times 10^6\mathrm{m}^3/\mathrm{s}$ respectively (Fig 3). This gives a timescale τ of 31 years for VCOMP and 24 years for SCOMP. The hosing decreases by 500 m^3/s every year, giving $\lambda = 1.4 \times 10^{-19}$ PSU/s^2 for both experiments

The predicted salinity change from this very simple model is shown in Fig 13 along with the actual salinity increase. The predicted salinity increases are of a similar order of magnitude to that in the FAMOUS experiments and show the salinity in VCOMP increasing faster than that in SCOMP. This can be traced to the difference in circulation strength between the two experiments which changes the timescale of adjustment. Since SCOMP has a stronger reverse circulation than VCOMP, the residence timescale in the region is smaller and the salinity initially increases more slowly.

References

de Boer AM, Toggweiler JR, Sigman DM (2008) Atlantic Dominance of the Meridional Overturning Circulation. J Phys Oceanogr 38(2):435–450, DOI 10.1175/2007jpo3731.1

Cimatoribus AA, Drijfhout SS, den Toom M, Dijkstra HA (2012) Sensitivity of the Atlantic meridional overturning circulation to South Atlantic freshwater anomalies. Climate Dynamics 39:2291–2306, DOI 10.1007/s00382-012-1292-5

Clement AC, Peterson LC (2008) Mechanisms of abrupt climate change of the last glacial period. Rev Geophys 46(4):RG4002+, DOI 10.1029/2006rg000204

Collins M, Knutti R, Arblaster J, Dufresne JL, Fichefet T, Friedlingstein P, Gao X, Gutowski WJ, Johns T, Krinner G, Shongwe M, Tebaldi C, Weaver AJ, Wehner M (2013) Long-term Climate Change: Projections, Commitments and Irreversibility. In: Stocker TF, Qin D, Plattner GK, Tignor M, Allen SK, Boschung J, Nauels A, Xia Y, Bex V, Midgley PM (eds) Climate Change 2013: The Physical Science Basis. Contribution of Working Group I to the Fifth Assessment Report of the Intergovernmental Panel on Climate Change, Cambridge University Press, Cambridge, United Kingdom and New York, NY, USA., DOI 10.1017/CBO9781107415324.025

Dee DP, Uppala SM, Simmons AJ, Berrisford P, Poli P, Kobayashi S, Andrae U, Balmaseda MA, Balsamo G, Bauer P, Bechtold P, Beljaars ACM, van de Berg L, Bidlot J, Bormann N, Delsol C, Dragani R, Fuentes M, Geer AJ, Haimberger L, Healy SB, Hersbach H, Hólm EV, Isaksen L, Kållberg P, Köhler M, Matricardi M, McNally AP, Monge-Sanz BM, Morcrette JJ, Park BK, Peubey C, de Rosnay P, Tavolato C, Thépaut JN, Vitart F (2011) The ERA-Interim reanalysis: configuration and performance of the data assimilation system. QJR Meteorol Soc 137(656):553–597, DOI 10.1002/qj.828

Drijfhout SS, Weber SL, van der Swaluw E (2011) The stability of the MOC as diagnosed from model projections for pre-industrial, present and future climates. Climate Dyn 37(7):1575–1586, DOI 10.1007/s00382-010-0930-z

Gent PR, McWilliams JC (1990) Isopycnal mixing in ocean circulation models. J Phys Oceanogr 20(1):150–155

Gordon C, Cooper C, Senior CA, Banks H, Gregory JM, Johns TC, Mitchell JFB, Wood RA (2000) The simulation of SST, sea ice extents and ocean heat transports in a version of the Hadley Centre coupled model without flux adjustments. Climate Dyn 16:147–16

Gregory JM, Saenko OA, Weaver AJ (2003) The role of the Atlantic freshwater balance in the hysteresis of the meridional overturning circulation. Climate Dynamics 21(7-8):707–717, DOI 10.1007/s00382-003-0359-8

Hawkins E, Smith RS, Allison LC, Gregory JM, Woollings TJ, Pohlmann H, de Cuevas B (2011) Bistability of the Atlantic overturning circulation in a global climate model and links to ocean freshwater transport. Geophys Res Lett 38, DOI 10.1029/2011GL047208

650 Hofmann M, Rahmstorf S (2009) On the stability of the Atlantic meridional
651 overturning circulation. Proceedings of the National Academy of Sciences
652 106(49):20,584–20,589, DOI 10.1073/pnas.0909146106
653 Holbourn A, Kuhnt W, Frank M, Haley BA (2013) Changes in Pacific
654 Ocean circulation following the Miocene onset of permanent Antarc-
655 tic ice cover. Earth and Planetary Science Letters 365:38–50, DOI
656 10.1016/j.epsl.2013.01.020
657 Hu A, Meehl GA, Han W, Abe-Ouchi A, Morrill C, Okazaki Y, Chikamoto
658 MO (2012) The Pacific-Atlantic seesaw and the Bering Strait. Geophys Res
659 Lett 39(3):L03,702+, DOI 10.1029/2011gl050567
660 Ingleby B, Huddleston M (2007) Quality control of ocean temperature and
661 salinity profiles - historical and real-time data. J Mar Sys 65:158–175
662 Jackson LC (2013) Shutdown and recovery of the AMOC in a coupled global
663 climate model: The role of the advective feedback. Geophysical Research
664 Letters 40(6):1182–1188, DOI 10.1002/grl.50289
665 Jackson LC, Schaller N, Smith RS, Palmer MD, Vellinga M (2013) Response of
666 the Atlantic meridional overturning circulation to a reversal of greenhouse
667 gas increases. Climate dynamics DOI 10.1007/s00382-013-1842-5
668 Jackson LC, Kahana R, Graham T, Ringer MA, Woollings T, Mecking JV,
669 Wood RA (2015) Global and European climate impacts of a slowdown of the
670 AMOC in a high resolution GCM. Climate Dynamics 45(11-12):3299–3316,
671 DOI 10.1007/s00382-015-2540-2
672 Johnson H, Marshall D, Sproson D (2007) Reconciling theories of a me-
673 chanically driven meridional overturning circulation with thermohaline
674 forcing and multiple equilibria. Climate Dynamics 29(7-8):821–836, DOI
675 10.1007/s00382-007-0262-9
676 Krebs U, Timmermann A (2007) Tropical AirSea Interactions Accelerate the
677 Recovery of the Atlantic Meridional Overturning Circulation after a Major
678 Shutdown. J Climate 20(19):4940–4956, DOI 10.1175/jcli4296.1
679 Kuhlbrodt T, Griesel A, Montoya M, Levermann A, Hofmann M, Rahmstorf
680 S (2007) On the driving processes of the Atlantic meridional overturning
681 circulation. Rev Geophys 45(2):RG2001+, DOI 10.1029/2004rg000166
682 Kuhlbrodt T, Rahmstorf S, Zickfeld K, Vikebø F, Sundby S, Hofmann M,
683 Link P, Bondeau A, Cramer W, Jaeger C (2009) An Integrated Assessment
684 of changes in the thermohaline circulation. Climatic Change 96(4):489–537,
685 DOI 10.1007/s10584-009-9561-y
686 Lenton TM, Marsh R, Price AR, Lunt DJ, Aksenov Y, Annan JD, Cooper-
687 Chadwick T, Cox SJ, Edwards NR, Goswami S, Hargreaves JC, Harris PP,
688 Jiao Z, Livina VN, Payne AJ, Rutt IC, Shepherd JG, Valdes PJ, Williams G,
689 Williamson MS, Yool A (2007) Effects of atmospheric dynamics and ocean
690 resolution on bi-stability of the thermohaline circulation examined using
691 the Grid ENabled Integrated Earth system modelling (GENIE) framework.
692 Climate Dynamics 29(6):591–613, DOI 10.1007/s00382-007-0254-9
693 Manabe BS, Stouffer RJ (1999) Are two modes of thermohaline circulation sta-
694 ble? Tellus A 51(3):400–411, DOI 10.1034/j.1600-0870.1999.t01-3-00005.x

695 Marotzke J, Willebrand J (1991) Multiple Equilibria of the Global Thermo-
696 haline Circulation. J Phys Oceanogr 21(9):1372–1385, DOI 10.1175/1520-
697 0485(1991)021%3C1372:meotgt%3E2.0.co;2
698 McManus JF, Francois R, Gherardi JM, Keigwin LD, Brown-Leger S
699 (2004) Collapse and rapid resumption of Atlantic meridional circula-
700 tion linked to deglacial climate changes. Nature 428(6985):834–837, DOI
701 10.1038/nature02494
702 McNeall D, Halloran PR, Good P, Betts RA (2011) Analyzing abrupt and
703 nonlinear climate changes and their impacts. WIREs Clim Change 2(5):663–
704 686, DOI 10.1002/wcc.130
705 Mecking JV, Drijfhout SS, Jackson LC, Graham T (2016) Stable AMOC off
706 state in an eddy-permitting coupled climate model. Climate Dynamics pp
707 1–16, DOI 10.1007/s00382-016-2975-0
708 Menviel L, Timmermann A, Elison Timm O, Mouchet A, Abe-Ouchi A,
709 Chikamoto MO, Harada N, Ohgaito R, Okazaki Y (2012) Removing the
710 North Pacific halocline: Effects on global climate, ocean circulation and the
711 carbon cycle. Deep Sea Research Part II: Topical Studies in Oceanography
712 61-64:106–113, DOI 10.1016/j.dsr2.2011.03.005
713 Menviel L, England MH, Meissner KJ, Mouchet A, Yu J (2014) Atlantic-Pacific
714 seesaw and its role in outgassing CO2 during Heinrich events. Paleoceanog-
715 raphy 29(1):58–70, DOI 10.1002/2013pa002542
716 Mikolajewicz U, Crowley TJ, Schiller A, Voss R (1997) Modelling telecon-
717 nections between the North Atlantic and North Pacific during the Younger
718 Dryas. Nature 387(6631):384–387, DOI 10.1038/387384a0
719 Okazaki Y, Timmermann A, Menviel L, Harada N, Abe-Ouchi A, Chikamoto
720 MO, Mouchet A, Asahi H (2010) Deepwater Formation in the North Pa-
721 cific During the Last Glacial Termination. Science 329(5988):200–204, DOI
722 10.1126/science.1190612
723 Rahmstorf S (1996) On the freshwater forcing and transport of the
724 Atlantic Thermohaline Circulation. Climate Dyn 12:799–811, DOI
725 10.1007/s003820050144
726 Rahmstorf S (2002) Ocean circulation and climate during the past 120,000
727 years. Nature 419(6903):207–214, DOI 10.1038/nature01090
728 Rahmstorf S, Crucifix M, Ganopolski A, Goosse H, Kamenkovich I, Knutti R,
729 Lohmann G, Marsh R, Mysak LA, Wang Z, Others (2005) Thermohaline
730 circulation hysteresis: A model intercomparison. Geophys Res Lett 32(23),
731 DOI 10.1029/2005GL023655
732 Roberts CD, Garry FK, Jackson LC (2013) A Multimodel Study of Sea
733 Surface Temperature and Subsurface Density Fingerprints of the Atlantic
734 Meridional Overturning Circulation. J Climate 26(22):9155–9174, DOI
735 10.1175/jcli-d-12-00762.1
736 Saenko OA, Schmittner A, Weaver AJ (2004) The AtlanticPa-
737 cific Seesaw. J Climate 17(11):2033–2038, DOI 10.1175/1520-
738 0442(2004)017%3C2033:tas%3E2.0.co;2
739 Schewe J, Levermann A (2010) The role of meridional density differences for a
740 wind-driven overturning circulation. Climate Dynamics 34(4):547–556, DOI

741 10.1007/s00382-009-0572-1
742 Schiller A, Mikolajewicz U, Voss R (1997) The stability of the North Atlantic
743 thermohaline circulation in a coupled ocean-atmosphere general circulation
744 model. Climate Dynamics 13(5):325–347, DOI 10.1007/s003820050169
745 Sévellec F, Fedorov AV (2011) Stability of the Atlantic meridional overturning
746 circulation and stratification in a zonally averaged ocean model: Effects of
747 freshwater flux, Southern Ocean winds, and diapycnal diffusion. Deep Sea
748 Research Part II: Topical Studies in Oceanography 58(17-18):1927–1943,
749 DOI 10.1016/j.dsr2.2010.10.070
750 Sinha B, Blaker AT, Hirschi JJM, Bonham S, Brand M, Josey S, Smith RS,
751 Marotzke J (2012) Mountain ranges favour vigorous Atlantic meridional
752 overturning. Geophys Res Lett 39(2):L02,705+, DOI 10.1029/2011gl050485
753 Smith RS, Gregory JM, Osprey A (2008) A description of the FAMOUS (ver-
754 sion XDBUA) climate model and control run. Geosci Model Dev 1:53–68,
755 DOI 10.5194/gmd-1-53-2008
756 Stommel H (1961) Thermohaline convection with two stable regimes of flow.
757 Tellus 13(2):224–230
758 Thomas DJ, Lyle M, Moore TC, Rea DK (2008) Paleogene deepwater mass
759 composition of the tropical Pacific and implications for thermohaline cir-
760 culation in a greenhouse world. Geochem Geophys Geosyst 9(2):Q02,002+,
761 DOI 10.1029/2007gc001748
762 Thorpe RB, Gregory JM, Johns TC, Wood RA, Mitchell JFB (2001) Mech-
763 anisms Determining the Atlantic Thermohaline Circulation Response to
764 Greenhouse Gas Forcing in a Non-Flux-Adjusted Coupled Climate Model.
765 J Climate 14:3102–3116
766 Vellinga M, Wood RA (2008) Impacts of thermohaline circulation shutdown in
767 the twenty-first century. Climatic Change 91(1):43–63, DOI 10.1007/s10584-
768 006-9146-y
769 Vellinga M, Wood RA, Gregory JM (2002) Processes Governing the Recovery
770 of a Perturbed Thermohaline Circulation in HadCM3. J Climate 15(7):764–
771 780, DOI 10.1175/1520-0442(2002)015%3C0764:pgtroa%3E2.0.co;2
772 de Vries P, Weber SL (2005) The Atlantic freshwater budget as a diagnos-
773 tic for the existence of a stable shut down of the Meridional Overturning
774 Circulation. Geophys Res Lett 32, DOI 10.1029/2004GL021450
775 Weaver AJ, Sedláček J, Eby M, Alexander K, Crespin E, Fichefet T, Philippon-
776 Berthier G, Joos F, Kawamiya M, Matsumoto K, Others (2012) Stability of
777 the Atlantic meridional overturning circulation: A model intercomparison.
778 Geophysical Research Letters 39(20), DOI 10.1029/2012GL053763
779 Weber SL, Drijfhout SS (2007) Stability of the Atlantic Meridional Overturn-
780 ing Circulation in the Last Glacial Maximum climate. Geophys Res Lett
781 34(22):L22,706+, DOI 10.1029/2007gl031437
782 Yin J, Schlesinger ME, Andronova NG, Malyshev S, Li B (2006) Is a
783 shutdown of the thermohaline circulation irreversible? J Geophys Res
784 111(D12):D12,104+, DOI 10.1029/2005jd006562

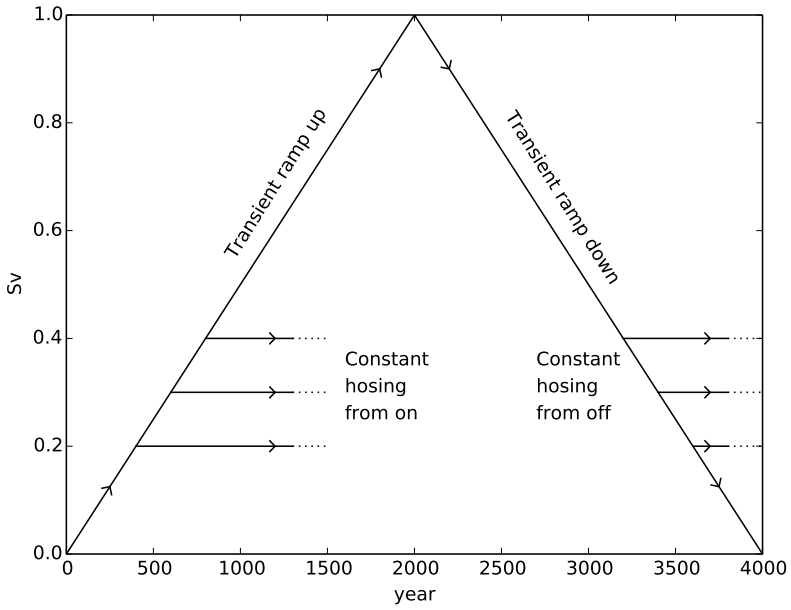

Fig. 1 Schematic of fresh water hosing applied over the North Atlantic in the transient hysteresis experiments (diagonal lines) and the equilibrium experiments with constant fluxes (horizontal lines). Experiments are described in Hawkins et al (2011).

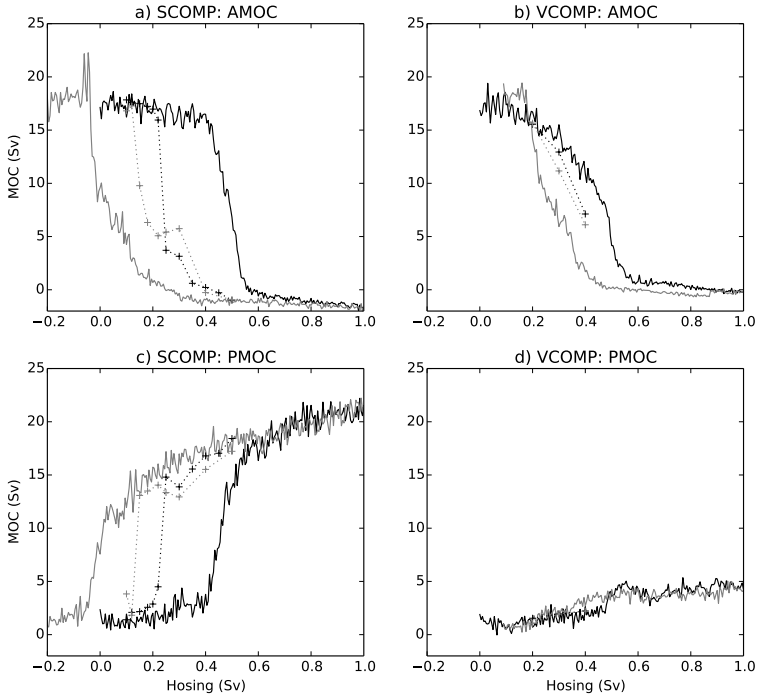

Fig. 2 Indices of AMOC (a,b) and PMOC (c,d) strength against hosing flux added to the North Atlantic for SCOMP (a,c) and VCOMP (b,d) experiments. Solid lines are the transient experiments and dotted lines with crosses show the final states of the constant hosing experiments. Black lines show experiments where hosing is ramped up, and gray lines show experiments where hosing is ramped down.

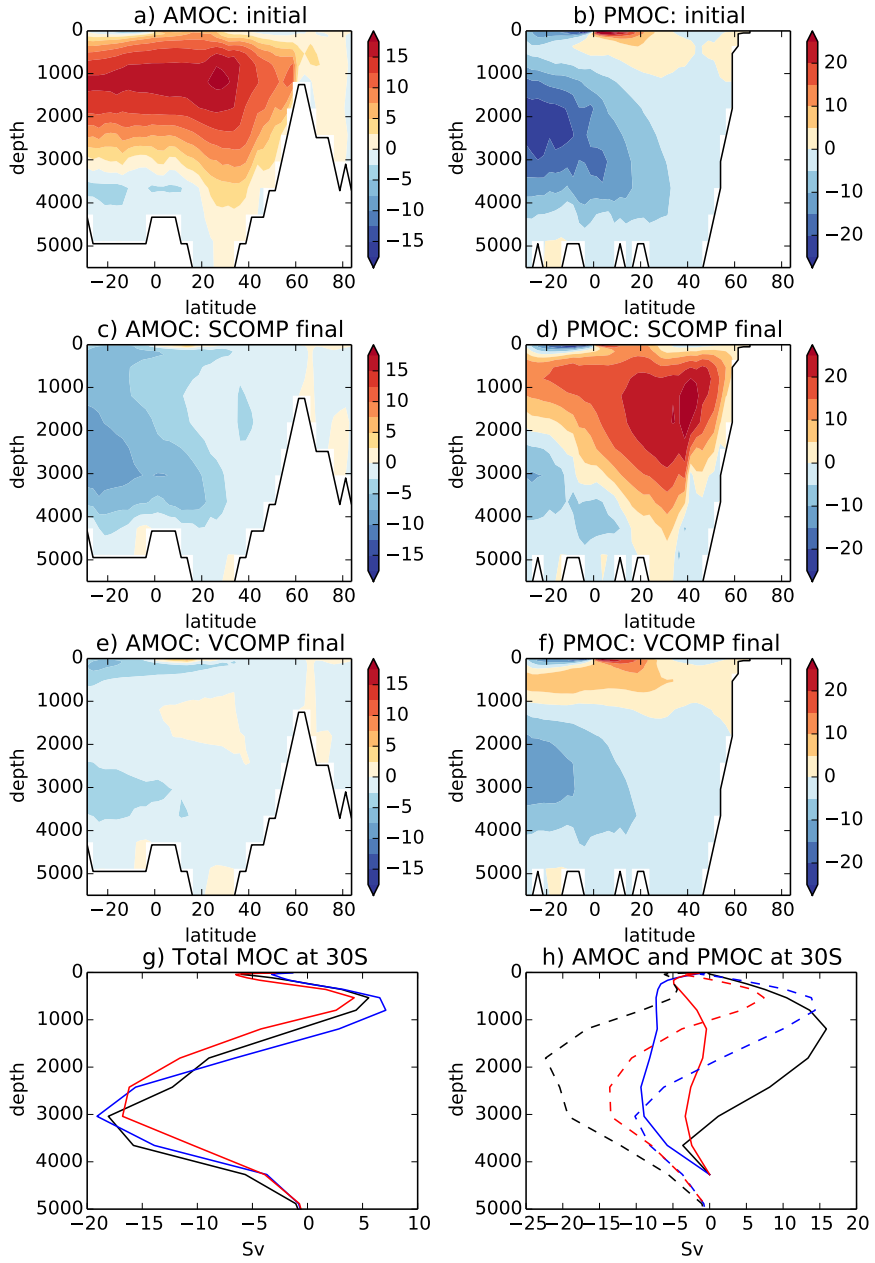

Fig. 3 Time mean overturning streamfunctions (Sv) for the Atlantic (a,c,e) and Indo-Pacific (b,d,f) for the SCOMP on state (year 0-200, a,b), the SCOMP off state (year 1800-2000, c,d) and the VCOMP off state (year 1800-2000, e,f). g) The global MOC (Atlantic plus Indo-Pacific) at 30°S for the SCOMP on state (black), the SCOMP off state (blue) and the VCOMP off state (red). h) As (g) except showing the values for the AMOC (solid lines) and PMOC (dashed lines).

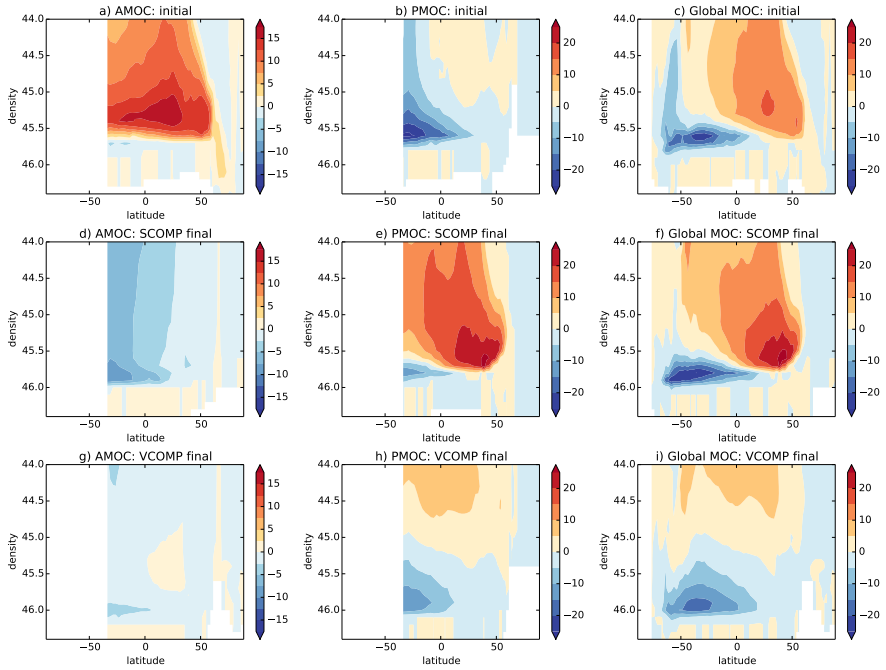

Fig. 4 Time mean overturning streamfunctions (Sv) for the Atlantic (a,d,g), Indo-Pacific (b,e,h) and globally (c,f,i) for the SCOMP on state (year 0-200, a,b,c), the SCOMP off state (year 1800-2000, d,e,f) and the VCOMP off state (year 1800-2000, g,h,i).

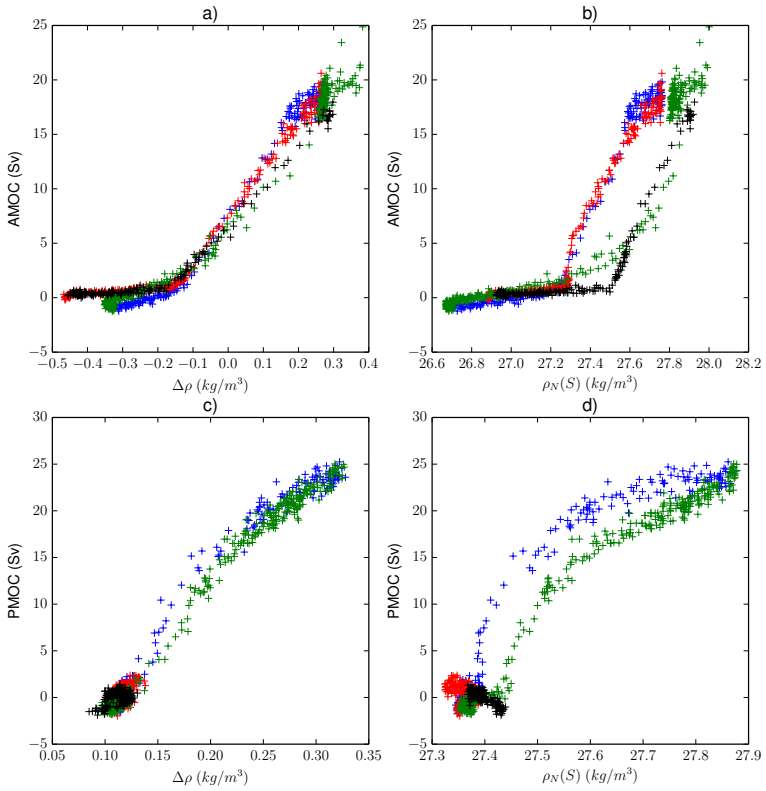

Fig. 5 Scatter plots of decadal mean MOC strength against (a,c) meridional density difference and (b,d) density in the north box due to salinity changes only. The regions used are (a,b) the Atlantic (density regions used are 40-90^{o}N and 20-35^{o}S) and (c,d) the Pacific (density regions used are 45-65^{o}N and 20-35^{o}S). Colors used are for the different experiments: SCOMP ramp up (blue), SCOMP ramp down (green), VCOMP ramp up (red) and VCOMP ramp down (black).

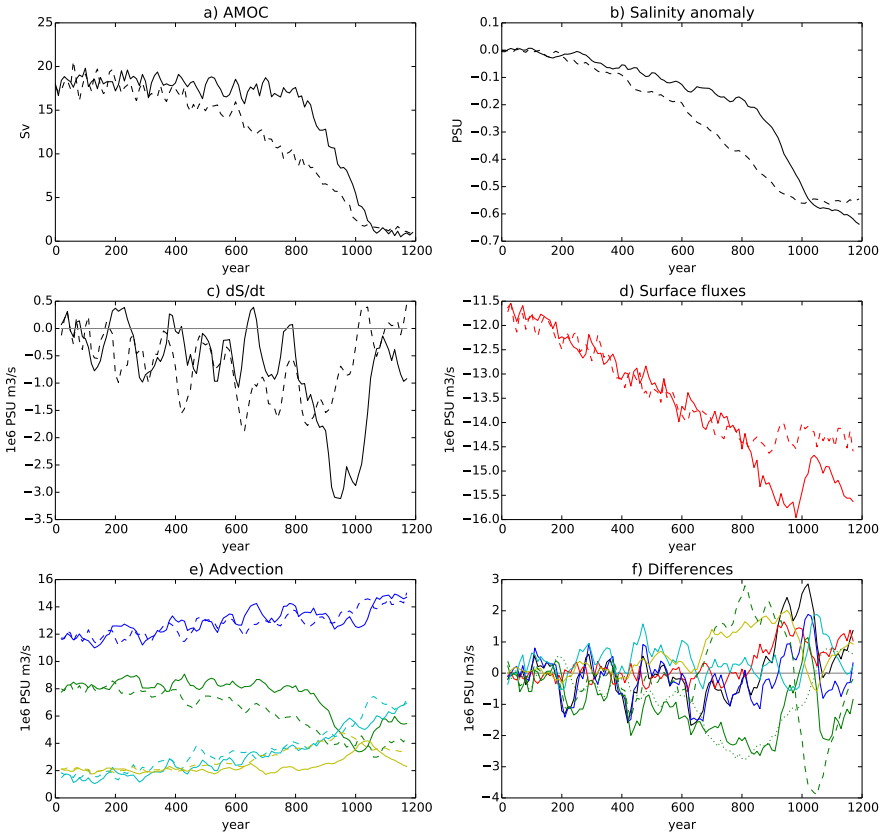

Fig. 6 Salinity budget of the North Atlantic during ramp up experiments with SCOMP (solid) and VCOMP (dashed). a) AMOC indices. b) salinity anomalies in the north Atlantic (40-90^{o}N). c) rate of change of salinity (black). d) surface fluxes including hosing (red). e) advection including total advection (blue), that from the overturning (green), that from the gyre circulation (cyan) and that from diffusion (yellow). f) budget terms in VCOMP minus those in SCOMP. The green dotted lines are the differences from advection of initial salinities by the anomalous overturning and the green dashed lines from advection of anomalous salinities by the initial overturning. Initial salinities and overturning are those from the on state (start of the ramp up experiment). Colors are as for the other panels. The black dotted lines in panels show the position of the x axis.

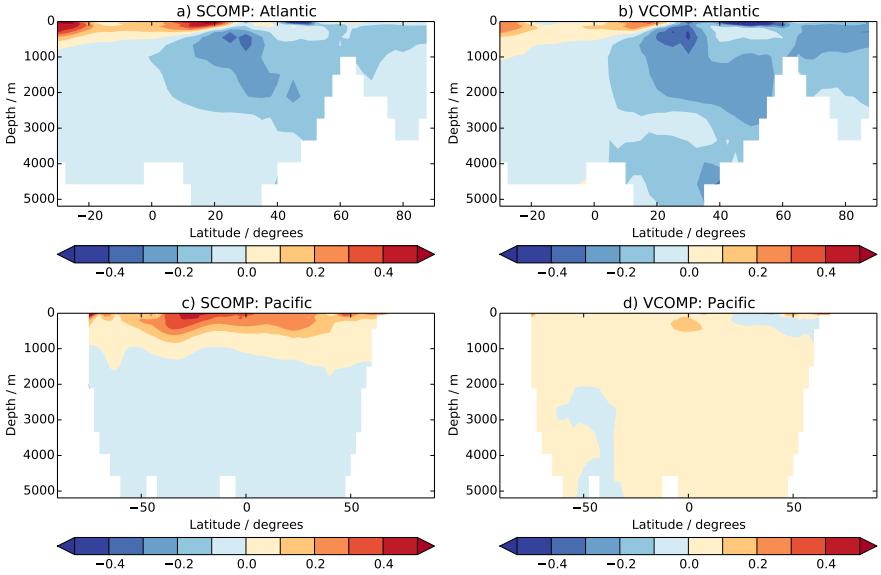

Fig. 7 Zonal mean sections of salinity anomalies in SCOMP (a,c) and VCOMP (b,d) in years 500-600 with respect to years 0-100 of the ramp up experiments for the Atlantic (a,b) and Pacific (c,d).

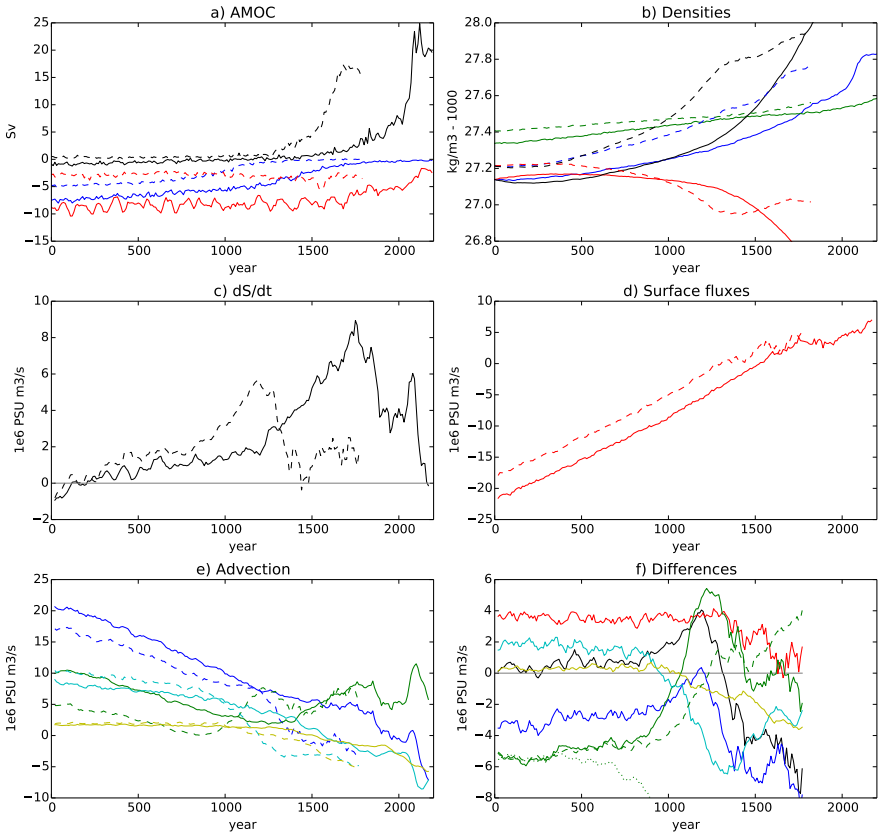

Fig. 8 Salinity budget of the North Atlantic during ramp down experiments with SCOMP (solid) and VCOMP (dashed). a) AMOC (black), AAIW (blue) and AABW (red) indices. b) densities in the north Atlantic (20-90^{o}N, blue) and south Atlantic (20-35^{o}S, green). Also shown are north Atlantic densities calculated with a time-evolving salinity and off state temperature (black) or time-evolving temperature and off state salinity (red). c) rate of change of salinity (black). d) surface fluxes including hosing (red). e) advection including total advection (blue), that from the overturning (green), that from the gyre circulation (cyan) and that from diffusion (yellow). f) budget terms in VCOMP minus those in SCOMP. The green dotted lines are the differences from advection of initial salinities by the anomalous overturning circulation and the green dashed lines from advection of anomalous salinities by the initial overturning circulation. 'Initial' salinities and overturning are those from the off state (start of the ramp down experiment). Colors are as for the other panels. The black dotted lines in panels show the position of the x axis.

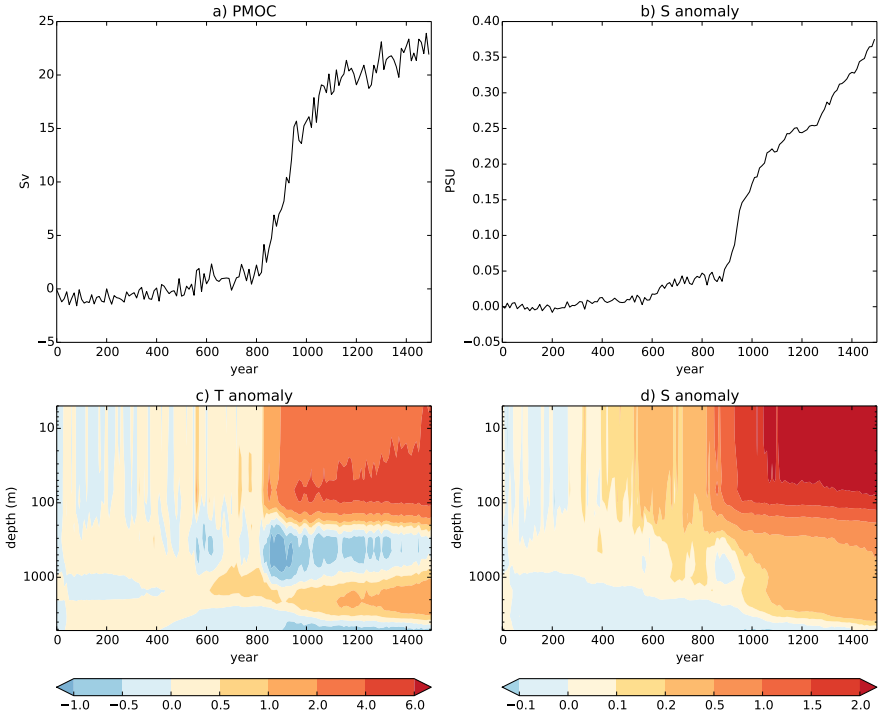

Fig. 9 a) The PMOC in SCOMP (Sv). b) The volume averaged salinity anomaly over the north Pacific box (45-65^{o}N, PSU). c) Temperature (^oC) anomalies (relative to years 0-100) area averaged over the north Pacific box. d) As c but for salinity anomalies (PSU). Note the nonlinear depth and contour scales.

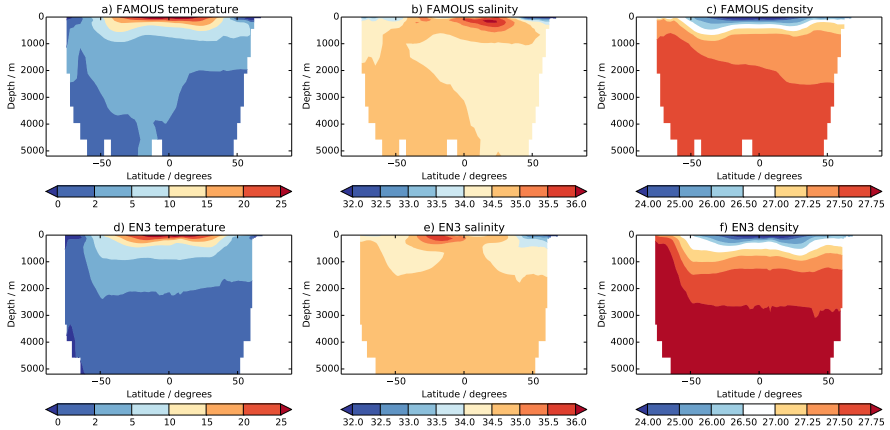

Fig. 10 Zonal mean sections of (a,d) temperature (^oC), (b,e) salinity (PSU) and (c,f) density (kg/m^3-1000) in the Pacific. (a,b,c) The fields from the initial model state (average of years 0-100 of SCOMP) and (d,e,f) values from the EN3 climatology (Ingleby and Huddleston, 2007)

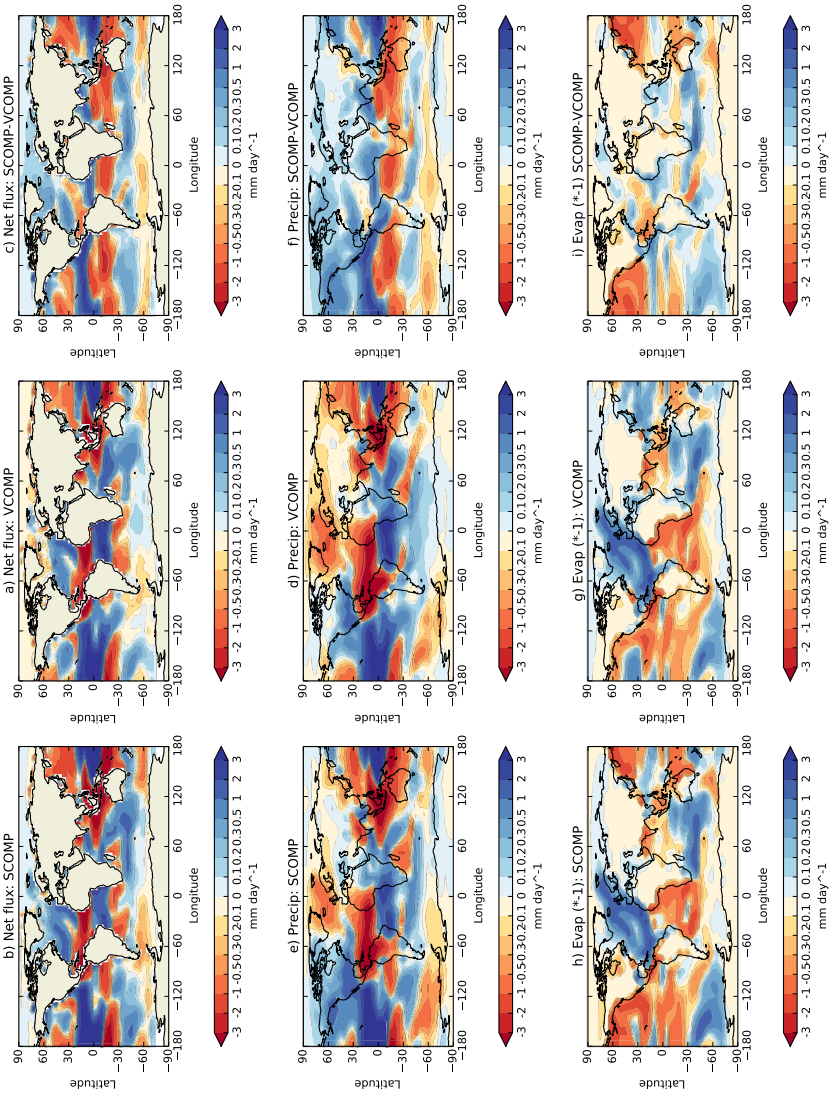

Fig. 11 Surface fresh water flux anomalies (years 1500-2000 average minus years 0-100 average) for SCOMP (a,d,g), VCOMP (b,e,h) and SCOMP-VCOMP (c,f,i). Shown are net flux into the ocean (precipitation - evaporation + runoff, a,b,c), precipitation (d,e,f) and (-1)*evaporation (g,h,i). Blue regions represent freshening by fluxes, and red regions represent salinification.

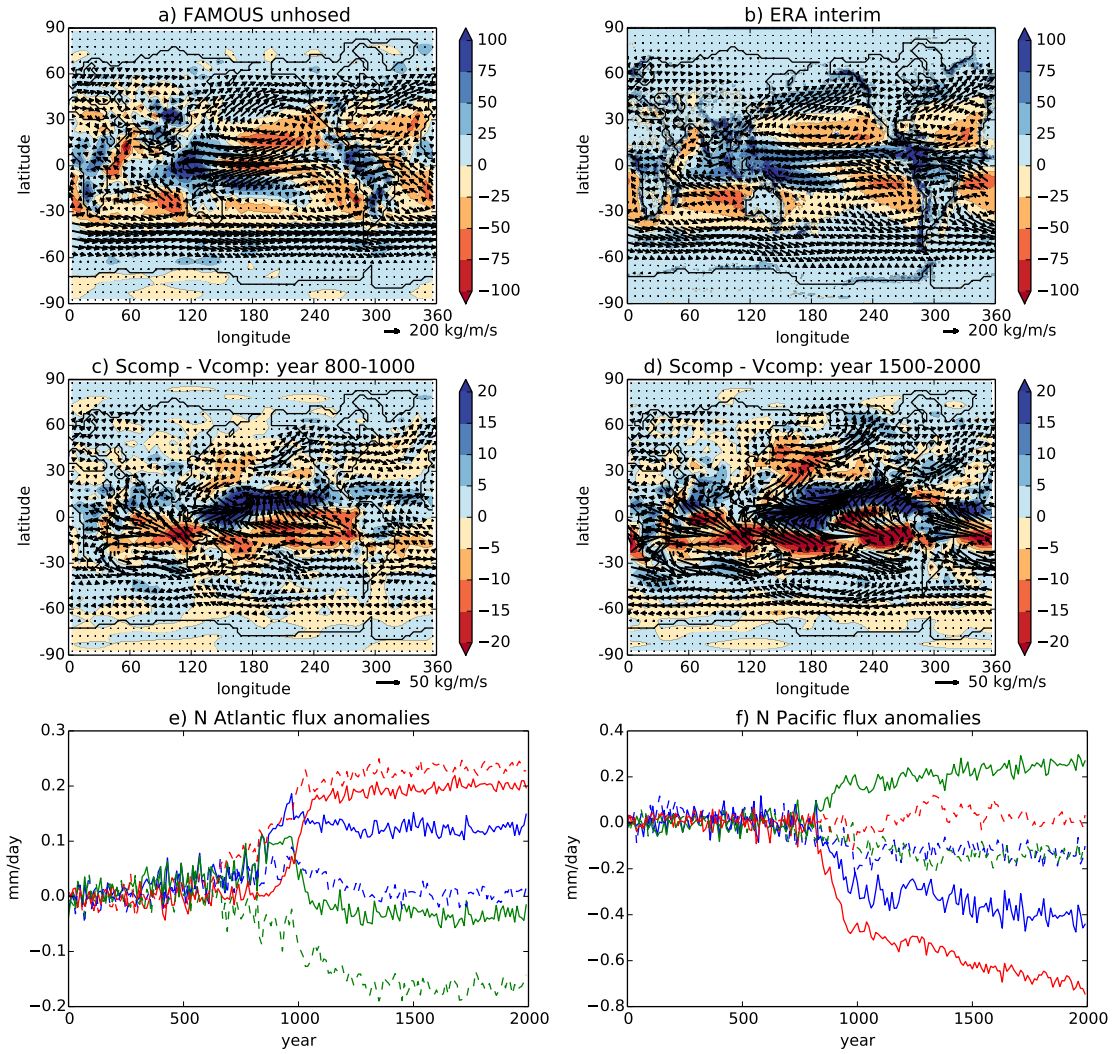

Fig. 12 Vertically integrated atmospheric moisture transport (arrows, in $kg/m/s$) overlying (-1×10^6)*moisture transport divergence ($kg/m^2/s$). a) moisture transport for the model initially (average of years 0-100 in SCOMP). b) Values from ERA interim. c) Difference between SCOMP and VCOMP in the years 800-1000. d) Difference between SCOMP and VCOMP when the AMOC is off (years 1500-2000). e) Time series of precipitation (green), (-1)*evaporation (red), net flux (precipitation-evaporation+runoff, blue) for SCOMP (solid) and VCOMP (dashed). Values are means over the North Atlantic (north of 65^{o}N and 40-65^{o}N, 90^{o}W-50^{o}E). f) As in the bottom left but for the North Pacific (30-65^{o}N, 110-250^{o}E).

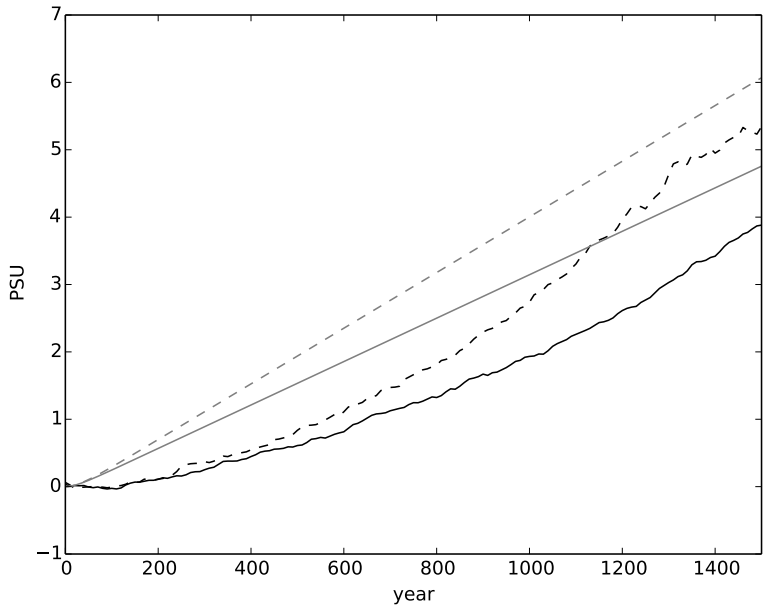

Fig. 13 Fig A1. Evolution of salinity anomalies in the upper North Atlantic over the region 0-500m, 20-60^{o}N from the AMOC off state. Shown are anomalies from the model experiments (black) and from the simple box model described in the Appendix (gray) for SCOMP (solid lines) and VCOMP (dashed lines).